34th Annual International Conference of the IEEE EMBS
San Diego, California USA, 28 August - 1 September, 2012

Vascular Stents with Rationally-Designed Surface Patterning

Shannon C. Gott, Benjamin A. Jabola, Guanshui Xu, and Masaru P. Rao, *Member, IEEE*

Abstract— **Herein, we discuss our recent progress towards realization of next-generation vascular stents that seek to mitigate adverse physiological responses to stenting via rational design of stent surface topography at the nanoscale. Specifically, we will discuss advances in patterning of deep sub-micrometer scale features in titanium (Ti) substrates, creation of cylindrical stents from micromachined planar Ti substrates, and integration of these processes to produce devices that will eventually allow evaluation of rationally-designed nanopatterning in physiologically-relevant contexts. We will also discuss results from mechanical testing and finite element modeling of these devices to assess their mechanical performance. These efforts represent key steps towards our long-term goal of developing a new paradigm for stents in which rationally-designed surface nanopatterning provides a physical means for complementing, or replacing, current pharmacological interventions.**

I. Introduction

Coronary heart disease (CHD) is the leading cause of death worldwide with an estimated death toll of 7.2 million men and women each year [1]. In the United States, approximately 1 in every 6 deaths is caused by CHD, with over 1 million people being affected by a coronary event each year [2]. The disease has also imposed a significant economic burden in the United States of more than $177 billion in 2007 [2]. It is evident that there is a need for a safe and effective solution to CHD.

CHD is a condition caused by atherosclerosis, which is characterized by chronic growth of plaque deposits beneath the endothelium, the innermost layer of cells in a vessel. This leads to the narrowing of blood vessels and subsequent restriction of oxygen-rich blood to the heart. One of the most common treatment methods for advanced CHD is to re-open the artery and push back the plaque-laden vessel walls with a stent. Stents are mesh-like cylindrical structures that are radially expanded at the site of vessel narrowing to maintain vascular patency. First generation stents, or bare-metal stents, were designed with purely mechanical functionality. Since then, second generation drug-eluting stents have revolutionized the field by reducing incidence of restenosis through local delivery of drugs that inhibit inflammation caused by implantation-induced injury. However, growing evidence suggests that this may also inhibit reestablishment of the endothelium, thus delaying healing and increasing potential for thrombogenic stimulus [3]. This, therefore, motivates the development of alternate therapeutic strategies that facilitate, rather than delay, healing.

As we first reported elsewhere [4,5], rational design of surface topography at the microscale may provide a new means for facilitating healing, thus increasing safety and efficacy. Specifically, our *in vitro* studies demonstrated that planar Ti substrates patterned with gratings composed of rectangular grooves ranging in width from 0.75 to 100 μm were able to increase endothelial migration and promote cellular morphology similar to that of the native endothelium, both of which would be expected to facilitate healing. Furthermore, we also demonstrated, for the first time, greatly enhanced competitive adhesion of endothelial cells over vascular smooth muscle cells, which suggests potential for inhibiting restenosis as well as facilitating healing. Finally, we observed favorable trending of these effects with decreasing feature size. Collectively, these results have provided the impetus for our recent efforts to push our surface patterning capability into the nanoscale realm, as well as to couple surface patterning with a more physiologically-relevant platform, i.e. the surface of stents.

II. Design and Fabrication

A. Design

Typically, stents are manufactured via laser-based micromachining of thin-wall tubular forms. However, laser micromachining does not provide sufficient resolution for realization of sub-micrometer to nano-scale surface patterning, thus necessitating exploration of other micromachining techniques. Recently developed deep reactive ion etching (DRIE) processes for bulk Ti substrates provide means for achieving such features [6,7]. However, the inherently planar nature of these processes necessitates development of means for creating cylindrical stents from planar substrates. Using an approach first reported by Takahata and Gianchandani for fabrication of stainless steel stents by microelectrodischarge machining [8], this limitation can now be circumvented.

Fig. 1 shows a schematic representation of a section of a planar stent consisting of transverse crossbands comprised of a series of s-shaped involute patterns connected by longitudinal side beams spanning the length of the stent. In order to produce the desired cylindrical geometry, the planar stent is first threaded onto a conventional balloon catheter such that each cross band is alternated in series above and below the balloon. The stent is then placed inside a 3 mm

S. C. Gott is with the Mechanical Engineering Department, University of California-Riverside, Riverside, CA 92521 USA (corresponding author: phone: 541-844-8238; e-mail: sgott@engr.ucr.edu).

B. A. Jabola, is with Saratech Inc., Lake Forest, CA 92630 USA (e-mail: AJabola@saratechinc.com).

Guanshui Xu is a Professor with the Department of Mechanical Engineering at the University of California-Riverside, Riverside, CA 92521 USA (e-mail: gxu@engr.ucr.edu).

M. P. Rao is an Assistant Professor with the Department of Mechanical Engineering at the University of California-Riverside, Riverside, CA 92521 USA (e-mail: mprao@engr.ucr.edu).

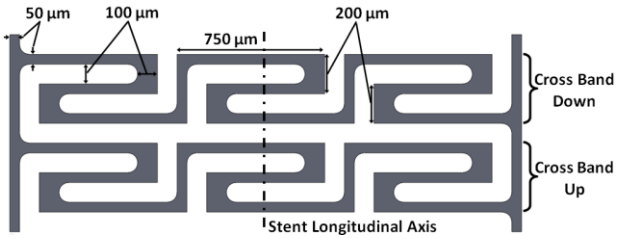

Figure 1. Design schematic for a small portion of a planar stent.

I.D. mock artery lubricated with silicone oil, and the balloon is inflated to 1.22 MPa, which is in the typical range for conventional stent deployment. During inflation, the stent undergoes plastic deformation via bending, rotation, and twisting of the crossbands and longitudinal side beams, thus allowing large deformations without tensile fracture. Fig. 2 illustrates this process and shows good stent strut uniformity after deployment.

B. Finite element analysis (FEA)

Elasto-plastic FEA was performed to simulate the stent deployment process, as well as subsequent mechanical testing via uniaxial radial compression. Both analyses were performed using the NX advanced simulation package (Siemens PLM, Cypress, CA) with a bilinear isotropic material model. Material properties used for Grade 1 Ti included: Young's modulus = 103 GPa; Poisson's ratio = 0.34; and yield strength = 170 MPa [9]. An estimated tangent modulus value of 297 MPa was used in both analyses, which was based upon the average slope of the engineering stress-strain curve over the plastic deformation regime. Finally, for both simulations, the stent geometry was simplified to a single pair of upper and lower crossbands to reduce computation time.

For the stent deployment simulation, the balloon was modeled as an expanding cylinder located within the lumen of the stent, and frictionless contact was assumed. In order to simplify the analysis, plastic deformation produced during the balloon threading process was ignored, and the initial configuration of the stent was assumed to be cylindrical with crossbands oriented as shown in Fig. 2 (left bottom micrograph). This simplification had only minor impact on the final results, since: a) Grade 1 Ti does not exhibit significant strain hardening; b) the majority of plasticity produced during threading and crimping is localized to the side beams; and c) the majority of plasticity produced during deployment is localized to the crossbands. Fig. 3 shows a typical simulation result, which returns maximum stresses below the ultimate tensile strength of the material (240 MPa [9]), in good agreement with experimental observations (i.e., there were no observations of crossband fracture in any stents deployed in this study).

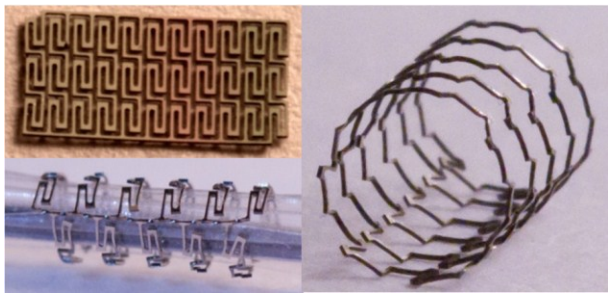

Figure 2. Left Top: Optical micrograph of planar Ti stent deep-etched through 80 µm Ti substrate. Left Bottom: Optical micrograph of planar Ti stent manually mounted and crimped onto conventional balloon catheter. Right: Optical micrograph of deployed Ti stent.

For the uniaxial radial compression simulation, the "balloon" was retracted and two parallel plates situated above and below the stent were used to impose 1.5 mm deformation (half the deployed diameter). Fig. 4 shows a typical simulation result, which returns a qualitative estimation of the actual uniaxial radial compression. Extraction of quantitative load-displacement data from these analyses show good agreement with experiments, as will be discussed in Section IV.

C. Fabrication

The Ti-based planar stents were fabricated from double-sided polished 80 µm thick Ti substrates (Grade 1 Ti, Tokyo Stainless Grinding Co.). The substrates were first solvent cleaned, followed by rinsing in DI water and N_2 drying. Next, as shown in Fig. 5, a thin SiO_2 etch mask was

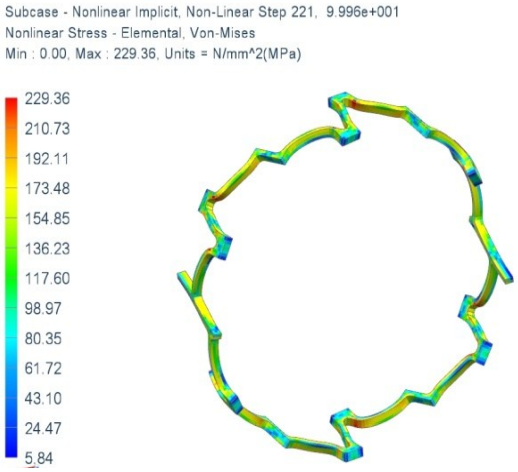

Figure 3. Von Mises stress plot for two bands of deployed planar Ti stent.

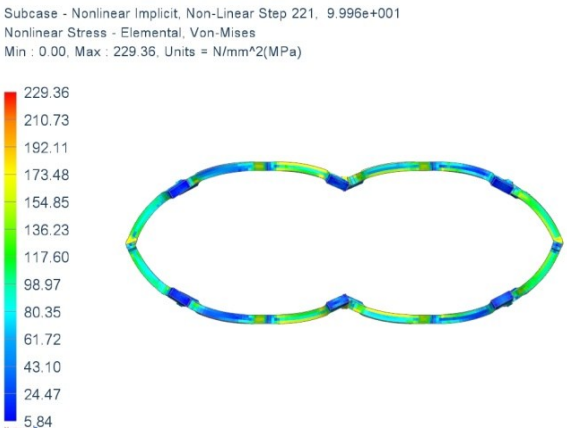

Figure 4. Deformation response of deployed planar Ti stent after 1.5 mm uniaxial radial compression.

deposited by ICP PECVD (VLR, Unaxis). The substrates were then briefly exposed to oxygen plasma, followed by photoresist (PR) application. The substrate was then brought into contact with a silicon-based imprint master, and a thermal imprinting process was performed (NX2000, Nanonex Inc.). To minimize PR adhesion, a monolayer coating of perflourodecyltricholorsilane was deposited on the imprint master using molecular vapor deposition (MVD 100E, Applied Microstructures, Inc.). After imprinting, the residual PR layer was removed using dry etching (E620-R&D, Panasonic Factory Solutions). Transfer of the imprinted PR pattern to the Ti substrate was then achieved via dry etching of the SiO_2 etch mask, followed by solvent cleaning to remove PR residue, application of a modified Ti DRIE process for shallow sub-micrometer scale patterns, and finally, removal of the residual SiO_2 via dry etching. As shown in Fig. 6, uniform gratings with depths on the order of 1 µm were produced.

Once the surface patterning was defined, the planar stent pattern was etched through the substrate from the back side. First, a thick ICP PECVD SiO_2 etch mask was deposited on the back side and the substrate mounted, surface pattern side down, to a Si carrier wafer with thermally conductive adhesive tape. Contact lithography was then used to define the stent pattern on the SiO_2, followed by dry etching through the SiO_2 layer and Ti to yield a planar stent.

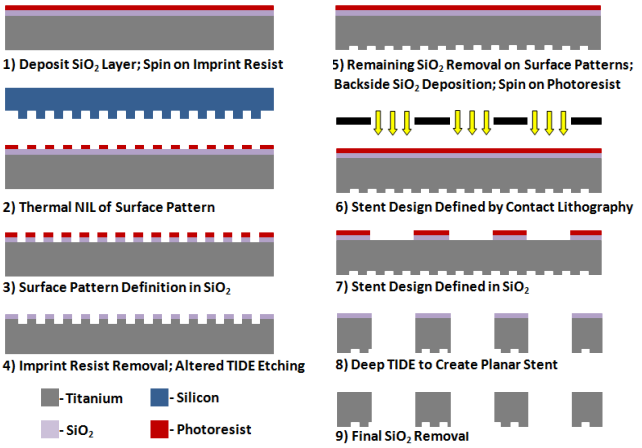

Figure 5. Fabrication process flow for sub-micrometer surface-patterned planar Ti stents.

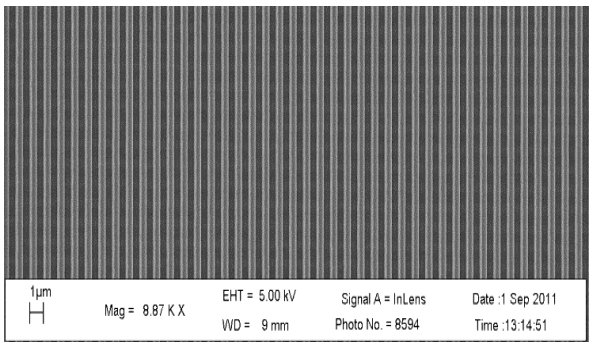

Figure 6. Scanning electron micrograph of 0.5 µm line width grating etched to ~1 µm depth in a planar Ti substrate.

Scanning electron micrographs in Fig. 7 of a deployed stent show the smooth vertical sidewalls and sub-micrometer surface patterning achieved using the Ti DRIE processes.

III. Mechanical Testing

Radial stiffness of the deployed stents was characterized via mechanical testing (ElectroForce 3100, Bose Corporation). Measurement of load-displacement behavior under uniaxial radial compression was performed for a variety of stent orientations (i.e., varying sidebar position relative to loading axis), although all yielded similar results. Devices were carefully observed to ensure no slipping occurred during testing. Resulting load-displacement data was compared to a planar stainless steel stent [8], as well as a commercial stainless steel stent [8], to serve as a reference standard. To allow for a direct comparison between differing stent designs, the loads were normalized by stent length.

IV. Results and Discussion

Fig. 7 demonstrates that stent integrity was maintained despite considerable deformation during deployment. Moreover, patterning was observed to have minimal effect on deformation response, with no evidence of cracking or tearing induced by patterning, even in instances where struts were excessively deformed due to non-uniform deployment. Finally, the robustness of the surface patterns themselves is evidenced by the absence of shearing or flattening observed across the deployed stents.

FEA modeling of stent deployment confirmed experimental observations that the maximum stresses lie below the threshold for tensile failure. This, therefore, provides initial validation of the model and its underlying assumptions. However, as shown in Fig. 8, the radial stiffness of the planar Ti stents is significantly lower than that of planar stainless steel stents of comparable design. Since the primary mechanical function of a stent is to maintain vascular patency, lower radial stiffness represents a

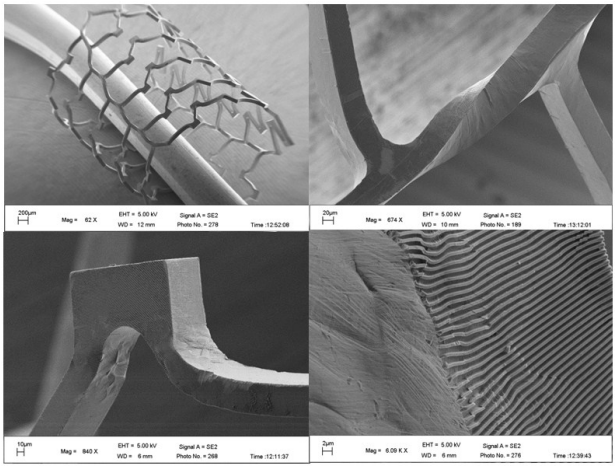

Figure 7. Scanning electron micrographs of a deployed surface-patterned Ti stent. Top left: Deployed stent. Top right: Two crossbands connecting to a sidebeam. Bottom left: Region of largest deformation and maximum stress (as indicated by FEA). Bottom right: Sub-micrometer scale gratings in a plastically deformed region.

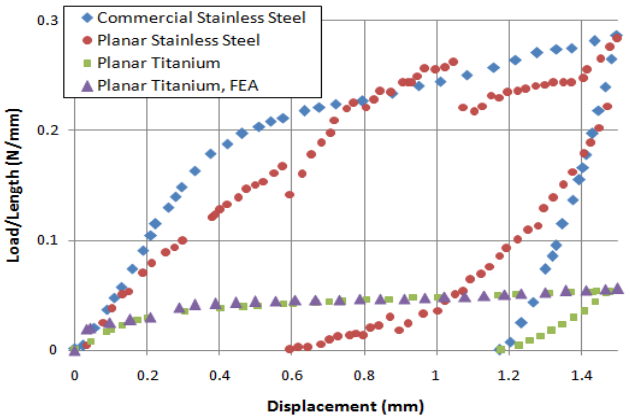

Figure 8. Normalized load-displacement data for stents under uniaxial radial compression: a) Commercial stainless steel stent, measured; b) Planar stainless steel stent, measured; c) Planar Ti stent, measured; and d) Planar Ti stent, FEA.

potential deficiency with regard to ultimate clinical efficacy. Moreover, lower stiffness could also introduce artifacts that adversely affect future studies evaluating cellular response to rationally-designed nanopatterning in more physiologically-relevant contexts, e.g., *in vitro* organ culture and small animal models. Consequently, this provides impetus to optimize our design to ensure comparable mechanical performance to that of commercial stainless steel stents.

The inferior stiffness of the planar Ti stents arises from both design and material-related deficiencies. For stents of identical design, substitution of Ti for stainless steel yields lower stiffness, since the elastic modulus for Grade 1 Ti is roughly half that of stainless steel (193 GPa) [9]. In the current study, substrate thickness was increased to compensate for this deficiency; however, the exact thickness required to do was difficult to estimate analytically, given the complex structural geometry. Moreover, there was only a limited range of substrate thicknesses from which to choose from. Consequently, 80 μm thickness was selected, which represents a 60% increase relative to the previously reported planar stainless steel stents [8]. The insufficiency of this thickness is clearly evident, thus motivating the subsequent development of the FEA radial compression model to help identify where design improvements could be made. The relatively good agreement between the simulated and measured response for the planar Ti stent suggests potential for performing virtual mechanical testing to allow evaluation of new designs in a more timely and cost-effective manner. Future efforts will focus on performing such analyses, as well as experimental validation of promising new designs.

V. Conclusion

We have reported the design, fabrication, mechanical testing, and finite element modeling of Ti stents with rationally-designed, sub-micrometer scale surface patterning. Realization of such stents required advancement of Ti DRIE capability, transformation of micromachined planar substrates into cylindrical stents, and integration of these processes to yield devices that will eventually allow juxtaposition of nanopatterned surfaces in the vascular wall in a manner consistent with stenting. While the mechanical response of these stents is currently inferior to that of commercial stents, elasto-plastic FEA models developed to simulate both stent deployment and radial compression show good agreement with experiments, thus suggesting opportunity for virtual design optimization and mechanical testing optimizing device design.

Acknowledgment

The authors would like to thank the staff at the UC Riverside and UC Santa Barbara Nanofabrication Facilities for assistance with device fabrication and process characterization. S.C.G. acknowledges the support provided by the National Science Foundation Graduate Research Fellowship Program.

References

[1] J. Mackay and G. A. Mensah, *The Atlas of Heart Disease and Stroke*. Geneva, Switzerland: World Health Organization, 2004, pp. 48-49.

[2] V. L. Roger, *et al.*, "Heart disease and stroke statistics – 2011 update: a report from the American Heart Association," *Circ* vol. 123, pp. e18-e209, Dec. 2011.

[3] M. Joner, A. V. Finn, A. Farb, E. K. Mont, F. D. Kolodgie, E. Ladich, R. Kutys, and K. Skorija, "Pathology of drug-eluting stents in humans," *J Am Coll Cardiol*, vol. 48, pp. 193-202, Mar. 2005.

[4] J. Lu, M. P. Rao, N. C. MacDonald, D. Khang, and T. J. Webster, "Improved endothelial cell adhesion and proliferation on patterned titanium surfaces with rationally designed, micrometer to nanometer features," *Acta Biomater* vol. 4, pp. 192-201, Jan. 2008.

[5] M. P. Rao, J. Lu, H. P. Aguilar, N. C. MacDonald, and T. J. Webster, in *Solid-State Sensors, Actuators, and Microsystems Workshop*, Hilton Head Island, SC, Jun. 2008.

[6] E. R. Parker, B. J. Thibeault, M. F. Aimi, M. P. Rao, and N. C. MacDonald, "Inductively coupled plasma etching of bulk titanium for MEMS applications," *J Electrochem Soc* vol. 152, pp. C675-C683, Aug. 2005.

[7] M. F. Aimi, M. P. Rao, N. C. MacDonald, A. S. Zuruzi, and D. P. Bothman, "High-aspect-ratio bulk micromachining of titanium," *Nat Mater* vol. 3, pp. 103-105, Feb. 2004.

[8] K. Takahata, and Y. B. Gianchandani, "A planar approach for manufacturing cardiac stents: design, fabrication, and mechanical evaluation," *J MEMS* vol. 13, pp. 933-939, Dec. 2004.

[9] W. D. Callister, Jr., *Materials science and engineering: an introduction*, 7th ed. New York: John Wiley & Sons, Inc., 2007, pp. A3-A36.